The Journal of Immunology

The NF-κB Canonical Pathway Is Involved in the Control of the Exonucleolytic Processing of Coding Ends during V(D)J Recombination

M. Margarida Souto-Carneiro, Ruth Fritsch, Nuno Sepúlveda, M. João Lagareiro, Nuno Morgado, Nancy S. Longo and Peter E. Lipsky

J Immunol 2008; 180:1040-1049; ;
doi: 10.4049/jimmunol.180.2.1040
http://www.jimmunol.org/content/180/2/1040

The Journal of Immunology is published twice each month by
The American Association of Immunologists, Inc.,
1451 Rockville Pike, Suite 650, Rockville, MD 20852

Print ISSN: 0022-1767 Online ISSN: 1550-6606.

The NF-κB Canonical Pathway Is Involved in the Control of the Exonucleolytic Processing of Coding Ends during V(D)J Recombination[1]

M. Margarida Souto-Carneiro,*† Ruth Fritsch,*‡ Nuno Sepúlveda,†§ M. João Lagareiro,† Nuno Morgado,† Nancy S. Longo,* and Peter E. Lipsky[2]*

V(D)J recombination is essential to produce an Ig repertoire with a large range of Ag specificities. Although NF-κB-binding sites are present in the human and mouse IgH, Igκ, and Igλ enhancer modules and RAG expression is controlled by NF-κB, it is not known whether NF-κB regulates V(D)J recombination mechanisms after RAG-mediated dsDNA breaks. To clarify the involvement of NF-κB in human V(D)J recombination, we amplified Ig gene rearrangements from individual peripheral B cells of patients with X-linked anhidrotic ectodermal dysplasia with hyper-IgM syndrome (HED-ID) who have deficient expression of the NF-κB essential modulator (NEMO/Ikkγ). The amplification of nonproductive Ig gene rearrangements from HED-ID B cells reflects the influence of the Ikkγ-mediated canonical NF-κB pathway on specific molecular mechanisms involved in V(D)J recombination. We found that the $CDR3_H$ from HED-ID B cells were abnormally long, as a result of a marked reduction in the exonuclease activity on the V, D, and J germline coding ends, whereas random *N*-nucleotide addition and palindromic overhangs (*P* nucleotides) were comparable to controls. This suggests that an intact canonical NF-κB pathway is essential for normal exonucleolytic activity during human V(D)J recombination, whereas terminal deoxynucleotide transferase, Artemis, and DNA-dependent protein kinase catalytic subunit activity are not affected. The generation of memory B cells and somatic hypermutation were markedly deficient confirming a role for NF-κB in these events of B cell maturation. However, selection of the primary B cell repertoire appeared to be intact and was partially able to correct the defects generated by abnormal V(D)J recombination. *The Journal of Immunology,* **2008, 180: 1040–1049.**

During B cell development, the variable domain of the Ig gene is assembled by randomly joining V, D, and J genes. This process is responsible for the production of a large repertoire of AgRs with a wide range of specificities (1), and the successful completion of this process is essential for B cell survival (2, 3). In the Ig molecule, the CDR3 is assembled from elements of the V and J gene segments and, in the case of the Ig H chain, also the D segment (4, 5), and is the most diverse region. This diversity is generated not only by the random recombination of V, D, and J elements, but also by the remarkable degree of processing of the joins by both nucleotide excision and addition. Structurally, the CDR3 is in the center of the Ag-binding site, interacting directly with the other CDRs and framework regions (FRs)[3] both from H and L chains, as well as with the Ag itself.

Many studies have linked NF-κB activity with B cell function and survival (6–13). For instance, IL-7-stimulated primary bone marrow B cells and an editing competent B cell line were unable to express RAG when cultured with inhibitors of the NF-κB/Rel family members, resulting in an impairment of L chain gene recombination (14). Furthermore, NF-κB-binding sites are present in the human and mouse IgH, Igκ, and Igλ enhancer modules (15–20). Different studies using mice or murine B cell lines have shown that impairing NF-κB function—either by knocking down/repressing its component subunits or by increasing IκBα expression—has dramatic effects on the level of Ig gene rearrangement (21–23). In vitro studies have demonstrated that the RAG proteins are critical in the joining phase of recombination and interact with the post-cleavage coding ends (24). However, in vivo, the role of NF-κB in regulating individual components of V(D)J recombination after initial RAG-mediated induction of DNA breaks directed to specific recombination signal sequences (RSS) of V, D, and J gene segments has not been delineated.

After RAG-mediated DNA cleavage, hairpin formation ensues creating a double-stranded break that must be resolved for successful V(D)J recombination. Several factors involved in DNA repair, including Artemis, DNA-dependent protein kinase catalytic subunit (DNA-PKcs), and Ku start processing and joining the coding ends (4, 25, 26). An unidentified 3′ to 5′ exonuclease activity removes nucleotides from the coding ends (27–30). Subsequently, the lymphocyte-specific enzyme terminal deoxynucleotide transferase (TdT) introduces nontemplated *N* nucleotides to the joins. Whether NF-κB might regulate some of these enzymatic processes is currently unknown.

Anhidrotic ectodermal dysplasia with hyper-IgM syndrome (HED-ID) is a rare X-linked primary immunodeficiency characterized by dysgammaglobulinemia and recurrent, mainly bacterial,

*Autoimmunity Branch, National Institute of Arthritis and Musculoskeletal and Skin Diseases, National Institutes of Health, Bethesda, MD 20892; †Instituto Gulbenkian de Ciência, Oeiras, Portugal; ‡Medical University of Vienna, Vienna, Austria; and §Center of Statistics and Applications, University of Lisbon, Lisbon, Portugal

Received for publication August 30, 2007. Accepted for publication November 5, 2007.

The costs of publication of this article were defrayed in part by the payment of page charges. This article must therefore be hereby marked *advertisement* in accordance with 18 U.S.C. Section 1734 solely to indicate this fact.

[1] This work was supported by the National Institute of Arthritis and Musculoskeletal and Skin Diseases Intramural Research Program. M.M.S.-C. was partially supported by the Marie Curie Intra-European Fellowship LIF-025885 and Fundação para a Ciência e Tecnologia Fellowship SFRH/BPD/20418/2004. N.S. was supported by Fundação para a Ciência e Tecnologia Fellowship SFRH/BD/19810. M.J.L. was supported by Instituto do Emprego e Formação Profissional and Fundação Calouste Gulbenkian.

[2] Address correspondence and reprint requests to Dr. Peter E. Lipsky, Autoimmunity Branch, National Institute of Arthritis and Musculoskeletal and Skin Diseases, National Institutes of Health, Room 6D47C, 9000 Rockville Pike, Bethesda, MD 20892-1560. E-mail address: lipskyp@mail.nih.gov

[3] Abbreviations used in this paper: FR, framework region; TdT, terminal deoxynucleotide transferase; HED-ID, anhidrotic ectodermal dysplasia with hyper-IgM syndrome; NEMO, NF-κB essential modulator; DNA-PKcs, DNA-dependent protein kinase catalytic subunit.

Table I. *Patients assessed*

	Age (Years)	Race	Ikkγ Mutation
Control	2–16	Caucasian ($n = 6$); Hispanic ($n = 2$); African American ($n = 4$)	None
HED-ID	2	Caucasian ($n = 1$)	C417Y
	7	Caucasian ($n = 1$)	D406V
	16	Caucasian ($n = 1$)	C417R
	17	Caucasian ($n = 1$)	C417R

infections starting in early childhood. HED-ID is caused by point mutations in the zinc finger motif of the highly conserved NF-κB essential modulator (NEMO/Ikkγ) (31–37). Ikkγ is a 48-kDa noncatalytic scaffolding protein for the IκB kinase (IKK) complex, which also contains the catalytic kinases Ikkα and Ikkβ (38, 39). This complex is an important inducer of NF-κB activity in immune or inflammatory responses. The activation of the IKK complex in response to TNF or LPS stimulation depends on the successful K63-linked TRAF2-dependent polyubiquitylation of the Ikkγ subunit followed by the phosphorylation of Ikkβ, resulting in IκB phosphorylation and subsequent NF-κB activation and translocation into the nucleus, where it binds its cognate sites on promoter/enhancer regions of target genes (38–40). More recently, it has been shown that Ikkγ also participates in virus-induced activation of IFN regulatory factors 3 and 7, through interaction with TRAF-associated NF-κB activator (TANK) (41). Studies on murine embryonic fibroblasts and human THP.1 monocytes expressing Ikkγ with C-terminal mutations demonstrated that the integrity of the Ikkγ C-terminal zinc finger motif is required for successful TNF-, IL-1-, or LPS-induced ubiquitylation of Ikkγ in response to inflammatory stimuli, and is also essential for Ikkβ-mediated phosphorylation of Ikkγ (42–45).

One way to examine the fine regulation of V(D)J recombination by NF-κB pathways of gene regulation is to study this process in individuals genetically deficient in NF-κB activation. By analyzing the CDR3 of Ig H and L chain genes of single B cells from peripheral blood of four HED-ID patients, we evaluated the role of the canonical NF-κB activation pathway in human V(D)J recombination. Amplification of Ig genes from genomic DNA of individual B cells permitted the assessment of nonproductive V(D)J rearrangements, which reflect the molecular mechanisms involved in recombination before selection. We found that the $CDR3_H$ from HED-ID B cells was abnormally long resulting from a marked reduction in the excision of the germline coding ends. The L chain coding ends also had a reduction in coding end excision, thus suggesting that, in humans, canonical NF-κB activation is required for the normal function of the exonucleolytic complexes participating in V(D)J recombination. In contrast, other enzymes involved in V(D)J recombination appeared to be intact, as was selection, that partially compensated for the defect in exonucleolytic excision.

Materials and Methods

Patient samples

Peripheral blood samples were collected from four Caucasian male patients with HED-ID with different hypomorphic mutations in the C-terminal region of the Ikkγ zinc-finger motif. Control blood samples were collected from 12 healthy age-matched controls (Table I). All blood collections and processing were done in accordance with policies established by the Institutional Review Board for human subjects at the National Institutes of Health (Bethesda, MD).

Flow cytometry and cell sorting

PBMC were isolated using a Ficoll gradient (Amersham) and stained with mAbs against human CD19, IgD, CD27, CD4, CD8, and CD45R0 (BD Biosciences), and analyzed with a four-color FACSCalibur (BD Biosciences). T cell subsets were analyzed using FlowJo (Tree Star). The B cell subsets $CD19^+/IgD^+/CD27^+$, $CD19^+/IgD^+/CD27^-$, and $CD19^+/IgD^-/CD27^+$ were sorted using a FACSDiva (BD Biosciences) or a Dako-Cytomation MoFlo into 5-ml tubes containing 500 μl of 1× PBS.

Table II. *Number of H and L chain V(D)J rearrangements used in this study*

	Number of Donors	Nonproductive	Productive	P:NP Ratio
H chain				
Control	12	56	385	6.9:1
HED-ID	4	72	280	3.9:1[a]
λ Chain				
Control	2	12	64	5.3:1
HED-ID	3	20	44	2.2:1[a]
κ Chain				
Control	3	18	32	1.8:1
HED-ID	3	18	12	0.7:1[a]

[a] Significant difference ($p < 0.05$) from control.

Amplification of the IgV H and L chains by single-cell PCR

Sorted B cells were diluted to a final concentration of 1–1.5 cells/5 μl of PBS, and then aliquoted into 96-well PCR plates containing 10 μl of lysis buffer (2× PCR buffer plus 0.4 mg/ml proteinase K; Sigma-Aldrich). Cells were lysed for 60 min at 56°C followed by a denaturation step of 95°C for 10 min to isolate genomic DNA. The total genomic DNA was amplified with an initial nontemplated primer extension preamplification PCR (23). Preamplified genomic DNA was amplified with the following external family specific IgV_H, IgVκ, or IgVλ forward primers: IgV_H1 and 7, 5′-ATG GAC TGS AYY TGG AGV RTC-3′; IgV_H2, 5′-ATG GAC ACA CTT TGC TMC ACR-3′; IgV_H3, 5′-GGR CTB HGC TGG VTT TTY CTY-3′; IgV_H4, 5′-TGG TTY TTC CTY CTS CTG GTG-3′; IgV_H5, 5′-ATG GGG TCA ACC GCC ATC CTY-3′; IgV_H6, 5′-CTC ATC TTC CTG CCC GTG CTG-3′; IgVκ123Ext, 5′-GCK CAG CTY CTS KKS CTS CTR-3′; IgVλ1Ext, 5′-ATG GCC TGS TYY CCT CTC YTC-3′; IgVλ2Ext, 5′-ATG GCC TGG GCT CTG CTS CTC-3′; IgVλ3Ext, 5′-ATG GCM TGG RYC VYW CTM YKB-3′ plus external reverse IgJ_H, IgJκ, or IgJλ primers IgJ_HExt, 5′-ACC TGA GGA GAC GGT GAC C-3′; IgJκ1–4Ext, 5′-TAC GTT TGA TCT CCA SCT TGG-3′; IgJκ5Ext, 5′-TAC GTT TAA TCT CCA GTC GTG-3′; IgJλExt, 5′-AGG ACG GTS ASC TKG GT-3′. An external touchdown PCR was conducted on a DNA Engine Tetrad peltier thermal cycler (MJ Research). The external PCR product was used to set up the nested PCR using internal family-specific IgV_H, IgVκ, or IgVλ forward primers: IgV_H1N, 5′-CCT ACG TGA GGT YTC CTG CAA GGC-3′; IgV_H2N, 5′-CAG RTC ACC TTG AAG GAG TCT-3′; IgV_H3N, 5′-GTC CAG TGT SAG GTG CAG C-3′; IgV_H4N, 5′-GGT GCA GCT GCA GGA GTC G-3′; IgV_H5N, 5′-AAA AAG CCC GGG GAG TCT CTG ARG A-3′; IgV_H6N, 5′-CAG GTA CAG CTG CAG CAG TCA-3′; IgVκ1N, 5′-GTG CCA GAT GTG MCA TCC RG-3′; IgVκ2N, 5′-GAT CCA GTG VGG ATR TTG TGA TG-3′; IgVκ3N, 5′-GTC TKT GTC TCC AGG GGA AAG AG-3′; IgVλ1–2N, 5′-CAG TCT GYC YTG ACK CAG CCD-3′; IgVλ3N, 5′-TAT GAG CTG ACW CAG CCA CYC-3′ plus the internal reverse IgJ_H, IgJκ, or IgJλ primers: $IgJ_H1/2/4/5N$, 5′-GTG ACC RTK GTC CCT TGG CCC-3′; $IgJ_H3/6N$, 5′-TGA CCA GGG TKC CM GGC CC-3′; IgJκ2N, 5′-CAG CTT GGT CCC CTG GCC AAA-3′; IgJκ5N, 5′-CCA GTC GTG TCC CTT GGC CG-3′; IgJλ1N, 5′-GGT SAC CTT GGT SCC AST KCC-3′; IgJλ23N, 5′-GGT CAG CTK GGT SCC TCC KCC-3′. PCR products were purified using the Performa 96-Well Standard Plate kit (Edge BioSystems) and sequenced with a model 3100 capillary sequencer (Applied Biosystems) using the Big DyeTerminator version 1.1 Cycle Sequencing kit (Applied Biosystems). The efficiency of amplification of V_H sequences was 90%.

Compilation of the database

The sequences analyzed included: 1) 441 H chain, 76 λ L chain, and 50 κ L chain sequences from healthy control peripheral blood B cells; 2) 352 H chain, 64 λ L chain, and 31 κ L chain sequences from HED-ID peripheral blood B cells (Table II). All sequences are available in GenBank with accession numbers Eu303341–Eu304234.

Sequence analysis

All rearrangements were matched to their closest germline counterparts using the Web-based program JOINSOLVER (46). Rearrangements were

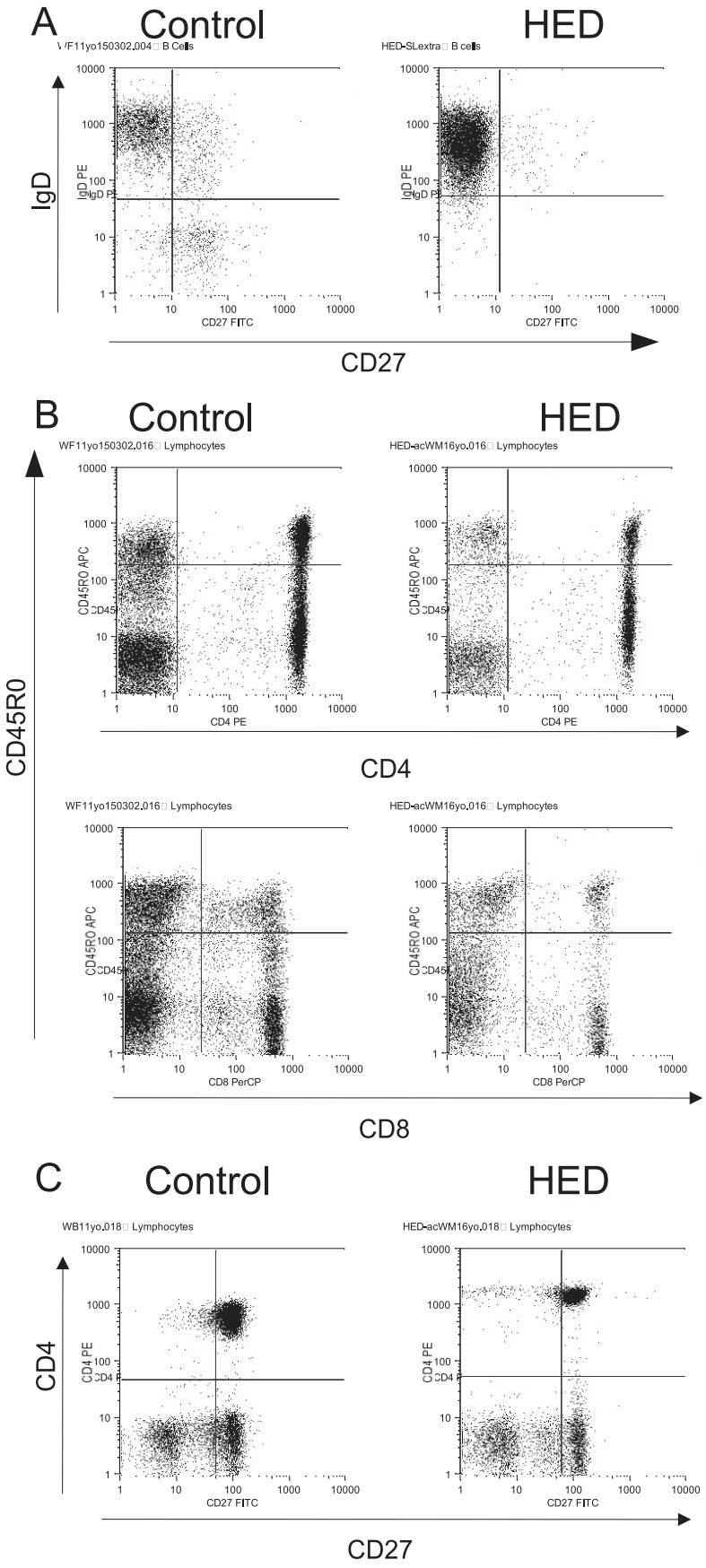

FIGURE 1. HED-ID patients have a reduced number of memory B cells, but normal levels of memory T cells when compared with age-matched controls. *A*, Peripheral blood $CD19^+$ B cells were stained with anti-IgD and -CD27 Abs to assess the percentage of $IgD^+/CD27^+$ and $IgD^-/CD27^+$ memory populations. *B*, Peripheral blood $CD4^+$ and $CD8^+$ T cells were stained with anti-CD45R0 Ab, to determine whether there were differences in T cell memory populations. *C*, Peripheral blood $CD4^+$ T cells were stained with anti-CD27 to determine whether CD27 expression by all cells was Ikkγ dependent. Results are representative of 4 HED-ID and 12 age-matched control samples.

considered productive if the V_HDJ_H, the $V_\lambda J_\lambda$, or the $V_\kappa J_\kappa$ junction maintained the reading frame into the J_H, the J_λ, or the J_k segment and contained no stop codons in the germline D segment or CDR3 junctions. Otherwise, rearrangements were considered nonproductive. Junctional nucleotide additions between the V_H and D, the D and J_H segments, the V_λ and J_λ or the V_κ and J_κ were scored as either *P* nucleotides, if they were inverted repeats

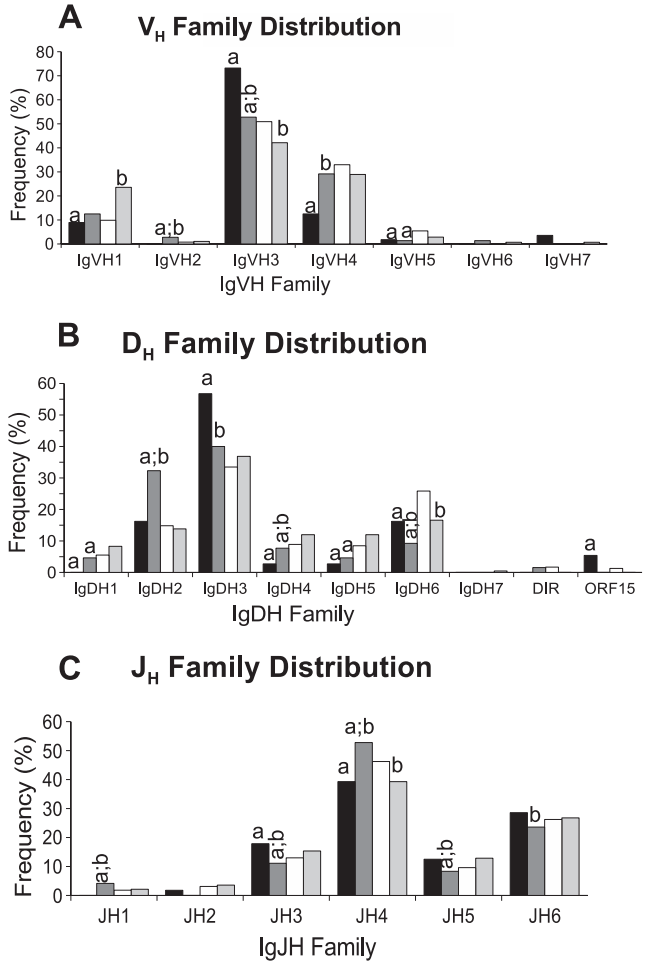

FIGURE 2. Distribution of the IgV_H (*A*), IgD_H (*B*), and IgJ_H (*C*) segments in HED-ID and control rearrangements. Frequency (percent) of control nonproductive (black bar), HED-ID nonproductive (dark gray bar), control productive (white bar), and HED-ID productive (light gray bar) rearrangements is represented. A total of 72 nonproductive and 280 productive rearrangements from patients with HED-ID and 56 nonproductive and 385 productive rearrangements from normal controls were analyzed. V_H, D_H, and J_H genes were identified with JoinSolver software (46), grouped into known families and the family distribution expressed as a percentage of the total rearrangements. Significant (*a*, $p < 0.05$) difference between productive and nonproductive rearrangements is shown. Significant (*b*, $p < 0.05$) difference when compared with controls.

of germline encoded ends, or *N* nucleotides, if they were nontemplated junctional additions. The junctions without *N* additions that contained base pairs that could have been encoded by either of the approximated coding ends, and therefore, could represent short regions of homology between the V_H and D, the D and J_H, the V_λ and J_λ, or the V_κ and J_κ regions were considered to be microhomologies. D segment matches and D segment fusions were only accepted when they fulfilled the criteria established previously (46), based on a Monte Carlo simulation designed to distinguish actual matches from random chance. In cases in which the nucleotide sequence between the V_H and J_H coding ends had the same number of matches with a D segment with irregular spacer (DIR) family member or a D segment encoded on chromosome 15 and a conventional D segment, the latter was accepted as the D element used. Rearrangements using DD fusions, inverted D segments, or D segment with irregular spacer segments were excluded from the D segment reading frame analysis.

Statistical analysis

To determine significant differences in distributions of productive and nonproductive rearrangements of V_H, D, and J_H segments in control and HED-ID cells, appropriate log-linear models for categorical data were fitted using the Catdata package (F. Z. Poleto and P. Rose, unpublished observations) for the R software (www.r-project.org/). A good fit of the models to data was considered when *p* values were <0.05 for Pearson's goodness-of-fit test. When stated, Fisher's exact tests were also applied to compare groups with respect to the frequency of a particular V_H, D, and J_H segment family and to analyze the productive:nonproductive ratio of H, λ, and κ chains in the two groups. The nonparametric Smirnoff-Kolgomorov test was used to compare the distributions of productive and nonproductive rearrangements, and of the control and HED-ID, regarding CDR3 length, V-J distance, D segment match length, *P* and *N* nucleotides, and V, D, and J excision. Here, *p* values <0.05 were considered to provide significant differences between two distributions.

Table III. *Frequency of rearrangements with unmatched D_H segments, mean $CDR3_H$ length, mean length of the D_H segment match, and V_H-J_H distance of the productive and nonproductive rearrangements (±SE)*

	Control (bp)	HED-ID (bp)
Nonproductive		
$CDR3_H$ length	55.6 ± 2.0[a]	63.1 ± 2.0[a,b]
V_H-J_H distance	39.5 ± 1.9[a]	44.2 ± 2.0[a,b]
D match length	17.0 ± 1.0[a]	19.2 ± 0.7[a,b]
No D match	33.9%	9.7%[a,b]
Productive		
$CDR3_H$ length	47.0 ± 0.6	50.3 ± 0.8[b]
V_H-J_H distance	28.4 ± 0.5	30.3 ± 0.6[b]
D match length	15.2 ± 0.3	16.7 ± 0.4[b]
No D match	39.2%	22.5%[b]

[a] Significant difference ($p < 0.05$) between nonproductive and productive rearrangements.
[b] Significant difference ($p < 0.05$) from control.

Results

HED-ID have a reduced and unmutated $IgD^+/CD27^+$ B cell population

The class-switched somatically mutated memory B cell subset ($CD19^+/IgD^-/CD27^+$) was present in all 12 control peripheral blood samples, but could not be detected in any of the HED-ID patients (mean HED-ID 0.8 ± 0.5% vs control 13.0 ± 1.5%). In two HED-ID patients, the $CD19^+/IgD^+/CD27^+$ preswitched memory B cell population was present, although it was significantly less frequent ($p < 0.05$) than in controls (Fig. 1*A*) (mean HED-ID 5.0 ± 3.9% vs control 12.1 ± 1.9%). When this $CD19^+/IgD^+/CD27^+$ B cell subset was analyzed for somatic mutations, the HED-ID IgV_H sequences were all unmutated contrasting to the extensive mutations observed in the same population from normals (data not shown). As a control, both CD4 and CD8 T cell subsets were analyzed for the expression of CD27 and CD45R0 to establish whether the Ikkγ mutation also influenced the memory phenotype of the T cell compartment and expression of CD27. The HED-ID peripheral blood T cells contained both $CD4^+$ and $CD8^+$ CD45R0-expressing memory populations comparable in frequency to the control subjects (Fig. 1*B*). Moreover, both T cell populations expressed CD27 (Fig. 1*C*).

Heavy chains

HED-ID H chain rearrangements. H and L chain gene rearrangements were amplified from genomic DNA of individual peripheral blood B cells of subjects with HED-ID and normal controls. This approach made it possible to amplify and analyze nonproductive rearrangements that reflect the immediate result of V(D)J recombination without subsequent selection as well as productive rearrangements, the distribution of which could have been influenced by selection (47).

Although the V_H segment distribution in productive and nonproductive rearrangements of HED-ID cells was statistically different from the controls ($p < 0.05$, Pearson's goodness-of-fit test), no major differences in individual V_H gene usage were observed (Fig. 2*A*). Thus, for example, even though there was a greater

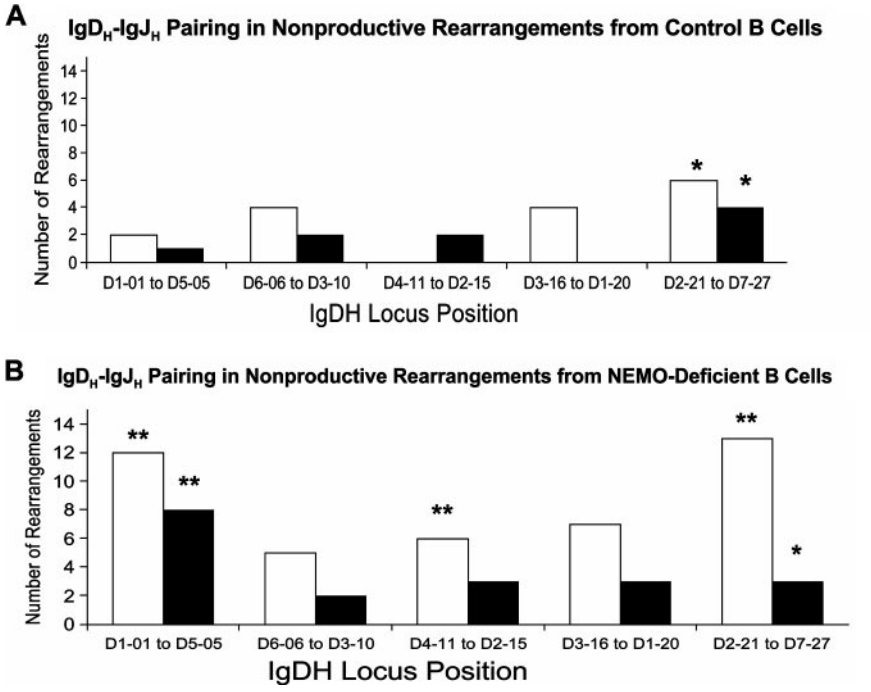

FIGURE 3. Pairing of IgD_H and IgJ_H segments in the nonproductive repertoire of the age-matched control (*A*) and the HED-ID (*B*) rearrangements. D proximal (□) J_H genes (J_H1, J_H2, J_H3, and J_H4) and D distal (■) J_H genes (J_H5 and J_H6) are indicated. The D genes are divided into five groups according to their position in the locus (D1–1 to D5–5 are the most J_H distal and D1–26 and D7–27 are the most J_H proximal). Significant (∗, $p < 0.05$) bias in the pairing of the D and J_H segments. Significant (∗∗, $p < 0.05$) difference when compared with controls. Only the rearrangements for which a D segment could be assigned were analyzed.

representation of the V_H4 family within the nonproductive HED-ID rearrangements compared with controls ($p < 0.05$, Fisher's exact test), this was not reflected in the overuse of a particular V_H4 family member (data not shown). Similarly, the increased representation of the V_H3 family in nonproductive rearrangements in HED-ID B cells was not the result of the overuse of any specific V_H3 gene. It is notable that HED-ID IgV_H rearrangements did not have any somatic hypermutation.

D segments could be matched significantly ($p < 0.05$) more often in both the nonproductive and productive HED-ID repertoires when compared with the control (Table III). Despite differences in the distribution of D segment family members, between HED-ID and normal V_H rearrangements, there were no significant changes in individual D segment usage. Differences between D segment usage between HED-ID and normal rearrangements was captured by a bad fit of a log-linear model assuming different probability distributions of D segments for productive and nonproductive rearrangements, but the same for control and HED-ID rearrangements (Pearson's goodness-of-fit test). Variance between HED-ID and normal in D segment usage could be accounted for by an increase in frequency of nonproductive D_H2 segments as well as by a decrease in frequency of productive D_H6 segments in HED-ID rearrangements, according to the good fit of a log-linear model assuming the same D segment distribution for control and HED-ID with the exception for the above-mentioned D segments, but different distribution for productive and nonproductive. Notably, the Ikkγ mutation was not related to an increased usage of chromosome 15 located D segments (Fig. 2*B*). Additionally, the reading frame usage was comparable between HED-ID and control repertoires (data not shown). Whereas the frequency of nonproductive rearrangements using multiple D segments was similar in HED-ID patients and controls (HED-ID 6.2% vs control 5.4%), in

Table IV. *Exonuclease activity in the V_HD or DJ_H junctions (±SE)*

	Control	HED-ID
Nonproductive		
V_H 3′ prime excision (bp)	3.0 ± 0.5^a	$2.0 \pm 0.4^{a,b}$
D 5′ prime excision (bp)	4.8 ± 0.6	3.9 ± 0.4
D 3′ prime excision (bp)	7.1 ± 1.1^a	4.5 ± 0.5^b
J_H 5′ prime excision (bp)	6.5 ± 0.5	5.0 ± 0.5^b
V_HD *P*-nucleotide addition (bp)	0.1 ± 0.1^a	0.4 ± 0.1^b
DJ_H *P*-nucleotide addition (bp)	0.03 ± 0.02^a	0.3 ± 0.1^b
V_HD with *P*-nucleotide addition (% of sequences)	$8.9\%^a$ ($n = 5$)	$25.0\%^b$ ($n = 18$)
DJ_H with *P*-nucleotide addition (% of sequences)	$3.6\%^a$ ($n = 2$)	$18.1\%^b$ ($n = 13$)
Productive		
V_H 3′ prime excision (bp)	1.8 ± 0.1	1.3 ± 0.1^b
D 5′ prime excision (bp)	5.2 ± 0.2	4.5 ± 0.2^b
D 3′ prime excision (bp)	4.7 ± 0.3	4.1 ± 0.3
J_H 5′ prime excision (bp)	5.6 ± 0.2	5.0 ± 0.3^b
V_HD *P*-nucleotide addition (bp)	0.3 ± 0.04	0.4 ± 0.05
DJ_H *P*-nucleotide addition (bp)	0.2 ± 0.03	0.2 ± 0.04
V_HD with *P*-nucleotide addition (% of sequences)	20.0% ($n = 77$)	27.5% ($n = 77$)
DJ_H with *P*-nucleotide addition (% of sequences)	10.1% ($n = 39$)	$17.1\%^b$ ($n = 48$)

[a] Significant difference ($p < 0.05$) between nonproductive and productive rearrangements.
[b] Significant difference ($p < 0.05$) from control.

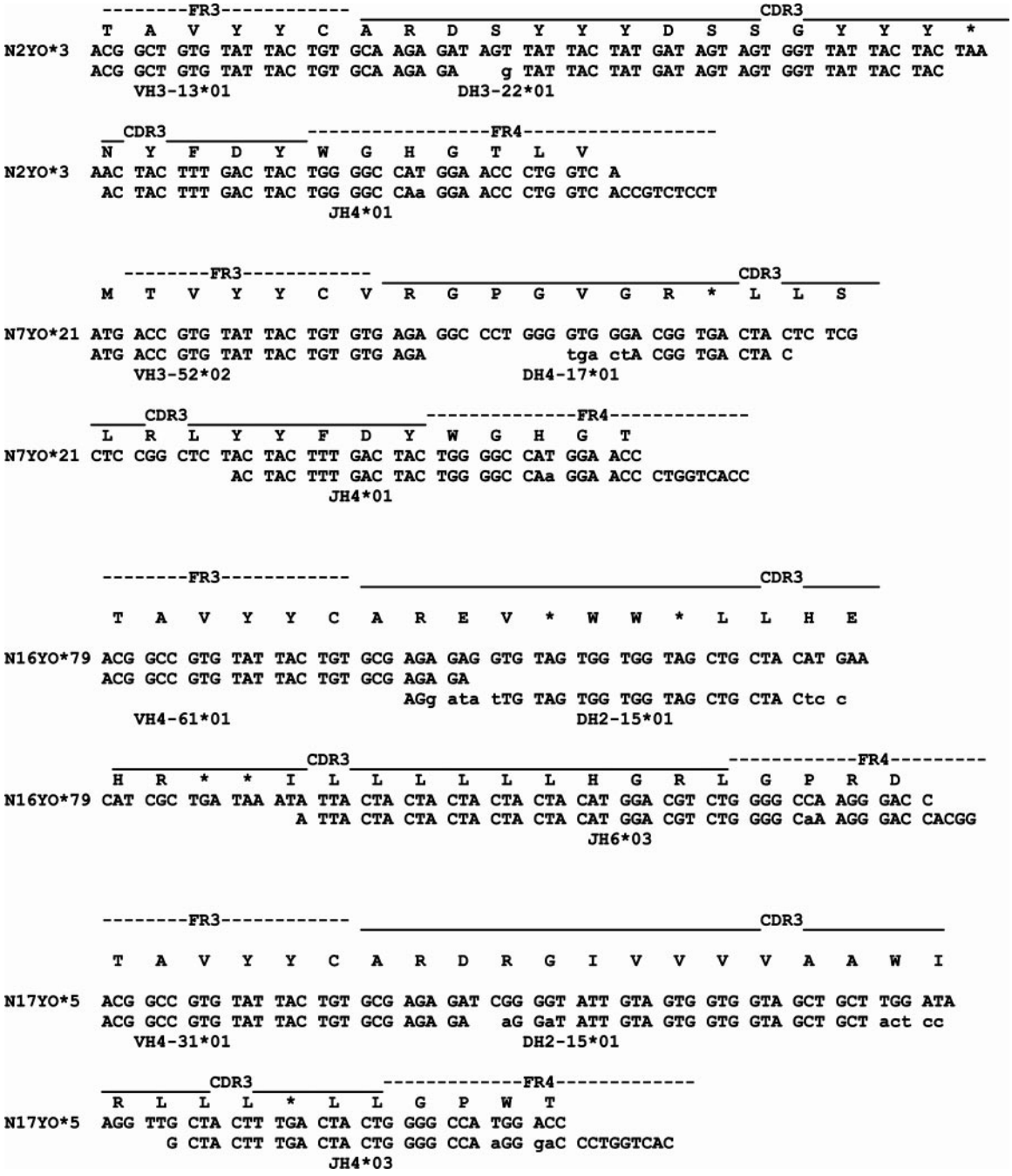

FIGURE 4. Alignment of the CDR3 region and the germline V_H, D, and J_H segments from selected nonproductive rearrangements from each of the patients with HED-ID. The $CDR3_H$ regions and the flanking $FR3_H$ and $FR4_H$ regions are shown. All four rearrangements are designated as nonproductive because of the insertion of STOP codons (indicated by an asterisk (*) in the amino acid sequence), or by additional shifting of the reading frame (N16YO*79 and N17YO*5). The entire 3′ portion of the relevant germline V_H segment, the 5′ portion of the relevant germline J_H segment, and the portion of the D segment included in the sequence are shown for each rearrangement. The corresponding IgV_H germline counterpart matches exactly the HED-ID sequence up to the last 3′ nucleotide of the germline gene in each rearrangement. This indicates that the exonucleolytic complexes did not cut back the HED-ID IgV_H gene when V_H to D-J_H recombination took place. Similarly, the HED-ID nucleotide sequence matches exactly all the nucleotides of the 5′ end of the IgJ_H germline gene in the $CDR3_H$ region, indicating that during the process of D to J_H recombination the exonucleases did not excise the coding ends. Homologous nucleotides between the germline and the HED-ID sequence are represented by capital letters. Nucleotide mismatches between the germline D segment and the HED-ID sequence are indicated by lowercase letters.

the productive repertoire there were significantly more ($p < 0.05$) HED-ID rearrangements using multiple D segments compared with control (HED-ID 2.8% vs control 0.8%).

Finally, the distribution of J_H segments in control and HED-ID nonproductive and productive rearrangements were similar in HED-ID and control B cells ($p = 0.12$, Pearson's goodness-of-fit test, Fig. 2*C*). Overall, these comparable distributions indicate that the Ikkγ mutation does not have a major impact on the choice and rearrangement of V_H, D, and J_H segments.

However, the ratios of productive to nonproductive rearrangements for the H and L chains were significantly lower ($p < 0.05$) for the HED-ID than for the controls (Table III). In addition, as shown in Fig. 3 there is a significant increase ($p < 0.05$) in recurrent D to J_H rearrangements in the HED-ID B cells in

Table V. *TdT activity in the V_HD, DJ_H, or V_HJ_H junctions (±SE)*

	Control	HED-ID
Nonproductive		
V_HD *N*-nucleotide addition (bp)	10.1 ± 1.0[a]	10.4 ± 0.8[a]
DJ_H *N*-nucleotide addition (bp)	12.2 ± 1.7[a]	14.8 ± 1.5[a]
V_HD with no addition (% of sequences)	5.4% ($n = 2$)	1.5%[b] ($n = 1$)
DJ_H with no addition (% of sequences)	8.1%[a] ($n = 3$)	1.5%[a,b] ($n = 1$)
Productive		
V_HD *N*-nucleotide addition (bp)	7.6 ± 0.3	7.4 ± 0.3
DJ_H *N*-nucleotide addition (bp)	7.4 ± 0.4	7.2 ± 0.4
V_HD with no addition (% of sequences)	4.7% ($n = 11$)	0.9%[b] ($n = 2$)
DJ_H with no addition (% of sequences)	14.1% ($n = 33$)	5.1%[b] ($n = 11$)

[a] Significant difference ($p < 0.05$) between nonproductive and productive rearrangements.
[b] Significant difference ($p < 0.05$) from control.

comparison to controls, as evidenced by the biased pairing of 5′D segments with 3′J segments.

HED-ID rearrangements have longer $CDR3_H$. The next experiments analyzed the $CDR3_H$ region of the H chain rearrangements from HED-ID subjects to determine whether the NEMO/Ikkγ mutation influenced specific elements of VDJ recombination. As shown in Table III, the mean $CDR3_H$ length of the HED-ID nonproductive rearrangements was significantly ($p < 0.05$) longer than in the control subjects (HED-ID 63.1 ± 2.0 bp vs control 55.6 ± 2.0 bp). A similar trend was evident in the productive repertoire, in which HED-ID rearrangements had significantly longer ($p < 0.05$) CDR3H than the control sequences (HED-ID 50.3 ± 0.8 bp vs control 47.0 ± 0.6 bp). Notably, in both the control and the HED-ID, the $CDR3_H$ length in the productive repertoire was significantly ($p < 0.05$) shorter than in the nonproductive. Analyses of the mean V_H-J_H distance demonstrated a significant increase in both the nonproductive and productive HED-ID rearrangements compared with normal. These results indicate that neither the V_H nor J_H segment contributed to the differences in the $CDR3_H$ length between the HED-ID and control.

The mean consecutive length of the nucleotide match between the analyzed VDJ rearrangements and the assigned germline D segments (Table III) was significantly longer ($p < 0.05$) in the HED-ID nonproductive repertoire than in the control B cells (HED-ID 19.2 ± 0.7 bp vs control 17.0 ± 1.0 bp). Even though the same trend could be observed in the productive repertoires (HED-ID 16.7 ± 0.4 bp vs control 15.2 ± 0.3 bp), the D segment match was significantly shorter ($p < 0.05$) in the productive compared with the nonproductive repertoire in both HED-ID and control, indicating that there is intact selection against long D segments in the HED-ID B cells. Finally, the nonproductive repertoire of both control and HED-ID B cells had significantly ($p < 0.05$) longer consecutive matches than the productive rearrangements. Overall, these results clearly indicate that rearrangements from HED-ID subjects have longer mean $CDR3_H$ than normal controls. Together with the finding reported above that the repertoire distribution in the HED-ID is similar to the healthy individuals, these results indicate that the differences in CDR3 length relate to abnormalities in V(D)J recombination and cannot be ascribed to differences of V, D, or J segment usage.

Exonuclease activity is reduced in HED-ID B cells. The next analyses sought to determine the basis of the long $CDR3_H$ in H chain rearrangements from subjects with HED-ID. Initially, we examined the imprint of exonuclease activity on V_H, D, and J_H segments. The D3′ and the J_H5' coding ends, as well as the V_H3' coding end, of the nonproductive HED-ID H chain repertoire underwent significantly less ($p < 0.05$) excision than the same coding ends of the control rearrangements (Table IV). Examples of HED-ID sequences with long $CDR3_H$ and diminished exonuclease activity are shown on Fig. 4. In contrast, the exonucleolytic activity on the HED-ID D5′ coding end of the nonproductive repertoire was comparable to that observed in the control rearrangements. Moreover, in the productive repertoire, the HED-ID V_H3', D5′, and J_H5' coding ends were excised significantly less than the controls. Furthermore, in the HED-ID nonproductive repertoire both the V_HD and DJ_H junctions contained a significantly greater ($p < 0.05$) frequency of inverted repeats at germline-encoded ends (*P* nucleotides) than the control sequences (Table IV). *P* nucleotides were more frequent in the V_H3', D5′, and J_H5' coding ends (data not shown). However, the mean length of these palindromic sequences was comparable between HED-ID and control. In the productive repertoire there were no detectable differences between the HED-ID and the control rearrangements.

HED-ID B cells have normal TdT activity. The next analyses examined the imprint of TdT activity on VDJ rearrangements from subjects with HED-ID. The addition of nontemplated nucleotides either in the V_HD or the DJ_H joint was significantly higher ($p < 0.05$) in nonproductive than in the productive repertoires, even though no differences were observed between the HED-ID and the control B cells (Table V). Even though there were significantly ($p < 0.05$) more V_HD and DJ_H junctions that did not have *N*-nucleotide additions in the controls compared with the HED-ID rearrangements in both productive and nonproductive repertoires, the usage of homologous coding end joining was comparable in the productive and nonproductive repertoires of HED-ID and control B cells (data not shown).

Table VI. *Mean $CDR3_\lambda$ length, V_λ-J_λ distance, TdT, and exonuclease activity in the λ rearrangements (±SE)*

	Control	HED-ID
Nonproductive		
$CDR3_\lambda$ length (bp)	33.8 ± 0.7[a]	32.8 ± 1.1
V_λ-J_λ distance (bp)	6.5 ± 1.7	2.2 ± 0.5[b]
$V_\lambda J_\lambda$ N-nucleotide addition (bp)	6.5 ± 1.7	2.2 ± 0.5[b]
V_λ 3′ prime excision (bp)	4.5 ± 1.1[a]	3.1 ± 0.7
J_λ 5′ prime excision (bp)	6.2 ± 1.5[a]	2.6 ± 0.6[b]
Productive		
$CDR3_\lambda$ length (bp)	31.8 ± 0.6	31.9 ± 0.4
V_λ-J_λ distance (bp)	7.3 ± 0.9	2.4 ± 0.6[b]
$V_\lambda J_\lambda$ N-nucleotide addition (bp)	7.3 ± 0.9	2.4 ± 0.6[b]
V_λ 3′ prime excision (bp)	8.1 ± 1.0	2.9 ± 0.5[b]
J_λ 5′ prime excision (bp)	2.6 ± 0.3	2.9 ± 0.4

[a] Significant difference ($p < 0.05$) between nonproductive and productive rearrangements.
[b] Significant difference ($p < 0.05$) from control.

Table VII. *Mean CDR3$_k$ length, V$_k$-J$_k$ distance, TdT, and exonuclease activity in the κ rearrangements (±SE)*

	Control	HED-ID
Nonproductive		
CDR3$_k$ length (bp)	26.1 ± 0.8[a]	27.1 ± 1.0
V$_k$-J$_k$ distance (bp)	5.1 ± 1.3	4.8 ± 1.5
V$_k$J$_k$ N-nucleotide addition (bp)	4.9 ± 1.3	4.4 ± 1.5
V$_k$ 3′ prime excision (bp)	7.2 ± 1.6[a]	3.1 ± 0.7[b]
J$_k$ 5′ prime excision (bp)	2.2 ± 0.5	2.6 ± 0.6
Productive		
CDR3$_k$ length (bp)	28.4 ± 0.3	28.4 ± 0.7
V$_k$-J$_k$ distance (bp)	3.8 ± 1.0	4.1 ± 1.2
V$_k$J$_k$ *N*-nucleotide addition (bp)	3.4 ± 1.0	3.8 ± 1.2
V$_k$ 3′ prime excision (bp)	5.1 ± 1.5	4.3 ± 1.2
J$_k$ 5′ prime excision (bp)	2.8 ± 0.5	1.8 ± 0.5

[a] Significant difference ($p < 0.05$) between nonproductive and productive rearrangements.
[b] Significant difference ($p < 0.05$) from control.

Light chains

No significant difference was observed in the usage of V segment families (V$_\kappa$1; V$_\kappa$2; V$_\kappa$3; V$_\lambda$1; V$_\lambda$2; and V$_\lambda$3), nor in the distribution of the J$_\kappa$ and J$_\lambda$ segments when the HED-ID and control κ and λ L chains were compared. In both the nonproductive and the productive κ and λ repertoires, no significant differences could be observed when comparing HED-ID CDR3 length to the controls (Tables VI and VII). Nonetheless, the J$_\lambda$5′ end of the HED-ID nonproductive λ repertoire was excised significantly less ($p < 0.05$) than in the control B cells (HED-ID 2.6 ± 0.6 bp vs control 6.2 ± 1.5 bp), and the V$_\lambda$3′ end of the HED-ID productive repertoire exhibited significantly less ($p < 0.05$) exonucleolytic cleavage than the control sequences (HED-ID 2.9 ± 0.5 bp vs control 8.1 ± 1.0 bp) (Table VI). However, whereas the excision of the V$_\lambda$3′ and J$_\lambda$5′ ends of the nonproductive control rearrangements were significantly different ($p < 0.05$) from the productive repertoire, the same was not observed in the HED-ID rearrangements, thus suggesting that selection was not able to correct abnormalities in exonucleolytic cleavage (Table VI). In the nonproductive HED-ID Vκ rearrangements, significantly decreased ($p < 0.05$) excision of the V$_\kappa$3′ end compared with control was observed, but no other significant differences could be observed in the excision of the coding ends (Table VII). Notably, all the HED-ID nonproductive κ rearrangements that did not exhibit V$_\kappa$3′ end excision had significantly longer ($p < 0.05$) CDR3κ than the rearrangements that were excised (29.0 ± 0.8 bp vs 27.1 ± 1.0 bp, respectively). These observations confirm the H chain results that there is a defect in exonuclease activity in the process of V(D)J recombination related to the hypomorphic point mutations in the Ikkγ zinc finger motif.

Discussion

In the present study, we used single-cell PCR to amplify Ig H and L chain genes from HED-ID B cells and demonstrated for the first time that mutations in the C-terminal zinc finger motif of the *Ikkγ* gene disturb the normal process of V(D)J recombination. Using this technique, both the nonproductive and the productive repertoires are amplified, allowing a clear separation of the immediate product of V(D)J recombination independent of the influences of selection (47). The molecular mechanisms of V(D)J recombination that are influenced by a functional canonical NF-κB pathway can be determined by analyzing the nonproductive repertoire. The present study provides strong evidence to suggest that impairment of the canonical NF-κB pathway while not influencing the apparent activity of TdT and DNA-PKcs during the process of V(D)J recombination, reduces the exonucleolytic processing of the coding ends. Particularly in the recombination of the H chain genes, this results in a significantly longer CDR3. However, selection partially corrected the defect in exonucleolytic processing, resulting in a lesser abnormality in the productive repertoire.

It is well-established that NF-κB regulates different aspects of B cell apoptosis (2, 9, 12), proliferation (10, 11, 48), maturation (6, 9, 13, 49–51), survival (8, 49, 52), class switch and Ig gene recombination (11, 14, 23, 35, 53–57). In vitro studies examining Ikkγ$^{-/-}$ embryonic stem cells cocultured with bone marrow cells (52) and in vivo studies using Mb-1Cre-transgenic mice lacking Ikkγ from the B cell progenitor stage on (48) defined a role for Ikkγ in the maturation and survival of B cells. Other studies in mice or murine cell lines presented evidence that defective (or absent) binding of NF-κB to its binding sites on the Ig gene enhancer modules reduced V$_\kappa$J$_\kappa$ and V$_\lambda$J$_\lambda$ rearrangements without influencing RAG gene expression (14, 22, 58), although others have reported a requirement for NF-κB expression in RAG upregulation and receptor editing (21).

However, such approaches do not mimic situations where Ikkγ is present but not fully functional as in HED-ID patients, nor provide information on the role of NF-κB in specific phases of the human V(D)J recombination process. Because the different stages of V(D)J recombination are well-correlated with the developmental stage of the B cells (59), analysis of the V(D)J rearrangements from peripheral blood HED-ID B cells allows an in-depth view of which molecular mechanisms are affected and the specific stages at which the canonical NF-κB pathway exerts an influence.

Previous studies have shown that NF-κB signaling is defective in B cells of HED-ID patients (50). In B cells, the NF-κB defect clearly resulted in a loss of memory B cells and an absence of somatic hypermutation. These results are consistent with previous findings that NF-κB plays an essential role in B cell maturation and survival.

In the naive B cell population, abnormalities in V(D)J recombination were also observed in the nonproductive repertoire. The abnormal CDR3$_H$ length was a direct result of reduced exonucleolytic processing of the germline coding ends, combined with intact TdT activity. In humans, TdT activity can be inferred from the mean number of *N*-nucleotide additions in the junctions (60–62). Our analysis yielded a comparable degree of TdT activity in the H chain rearrangements from HED-ID patients and control children which was similar to what was previously reported for adults (46, 47, 63). The TdT activity was also identical in the κ L chains of HED-ID and controls. This normal TdT activity in H and κ L chains was associated with a reduced usage of homologous coding end joining.

The number of nucleotides removed from the germline coding ends indicates the level of exonuclease activity that occurred before germline ends were joined. The HED-ID H chain rearrangements had fewer nucleotides excised from the V$_H$3′, D5′, and J$_H$5′ ends than the controls. However, there were no differences in the length of the palindromic overhangs between the HED-ID and the control rearrangements, suggesting that NF-κB is not involved in the control of DNA-PKcs and Artemis activities that control this (4, 64, 65). We could also observe reduced exonucleolytic activity on the coding ends of the HED-ID L chains. Taken together, this suggests that NF-κB is involved in controlling the exonuclease activity in B cells during V(D)J recombination. Because the DJ$_H$ junction is already present in the common lymphoid progenitor (66), the data indicate that a functional Ikkγ and a normal canonical NF-κB pathway are essential at this early stage of B cell development for the induction of normal exonuclease activity. Because the precise nature of the exonuclease involved in V(D)J

trimming is not known, whether NF-κB regulates its activity directly or indirectly it is not known. It is, however, interesting to note that exonuclease activity is the only process of V(D)J recombination to be sufficiently dependent on NF-κB to be observed to be clearly deficient in HED-ID B cells.

Additional abnormalities were noted in the Ig repertoire of HED-ID patients that might reflect a role for NF-κB signaling in B cell maturation. The first was a lower than normal ratio of productive to nonproductive rearrangements. For a nonproductive rearrangement to appear in the repertoire, it is essential that the specific B cell subsequently rearrange the allele on the opposite chromosome productively. Although it is commonly thought that each B cell routinely rearranges both Ig H chain loci, which would yield a productive to nonproductive ratio of 2.5, this is not the case as this ratio is usually much higher as found here (6.9 in controls) and previously (47). This implies that most B cells do not rearrange the second Ig H chain locus after an initial nonproductive V(D)J rearrangement. However, the productive to nonproductive ratio of the HED-ID V_H and V_λ rearrangements of 3.9:1 and 2.2:1, respectively, indicates that B cell maturation may have been altered by the defective NF-κB signaling so that more frequent rearrangements of the Ig loci on both chromosomes occurred. Deregulation of RAG expression owing to defects in NF-κB signaling may contribute (14). Alternatively, diminished proliferative capacity of pre-B cells owing to defective NF-κB signaling could slow the process of B cell maturation and make it more likely that rearrangements would occur on both chromosomes. Because Vκ genes can rearrange by deletion and inversion (1, 5), the lower productive to nonproductive ratio does not imply that both V_κ loci are normally rearranged more frequently. Notably, the productive to nonproductive ratio of V_κ rearrangements in HED-ID is also decreased consistent with the conclusion that the second Vκ locus is also rearranged more frequently when NF-κB signaling is diminished.

A second abnormality related to the degree of recurrent DJ_H rearrangement that occurred before V_H to DJ_H rearrangement. HED-ID rearrangements exhibited a greater tendency to rearrange 5′D segments to 3′J_H segments compared with control children, but similar to adult rearrangements. This suggests that HED-ID B cells undergo increased rounds of DJ_H rearrangements between the common lymphoid precursor and the pre-B cell stage before a final V_H to DJ_H recombination occurs. Furthermore, because defects in the canonical NF-κB-signaling pathway caused by p50-subunit deficiency can lead to RAG enzyme overexpression (14), it is possible that increased expression of RAG contributes. Whether abnormalities in RAG expression or alteration in B cell maturation because of defective NF-κB-signaling contributes to these abnormalities remains to be determined.

In previous reports, we and others have shown that selection tends to choose rearrangements with shorter $CDR3_H$ (46, 47, 67). It is notable that selection in HED-ID patients seems to be intact, because we observed a significant reduction in the $CDR3_H$ length in the productive repertoire. However, the mean $CDR3_H$ length never reached normal ranges because the reduced coding end excision and the elevated use of multiple D segments were never fully corrected. Because the $CDR3_H$ is located in the core of the Ag-binding pocket, it is possible that this extra length might compromise the binding of the Ag, thus partially contributing to the immunodeficiency observed in HED-ID patients.

It is noteworthy to mention that in our study, we confirmed previous observations that HED-ID patients are unable to switch their Ig and undergo somatic hypermutation (35, 36, 50). Nevertheless, we could detect in some patients a small B cell population with the $IgD^+/CD27^+$ phenotype that is typically associated with somatically mutated unswitched memory B cells (68), but lacking somatic mutations of the Ig genes. It is, therefore, possible that these B cells are not fully functional as memory B cells, and thus cannot protect HED-ID patients from recurrent bacterial infections. Importantly, the lack or significantly reduced CD27 expression on B cells in the HED-ID patients did not influence the level of CD70 expression on T cells (data not shown), nor was the T cell memory compartment reduced in these patients when compared with the healthy controls, perhaps affording a measure of host defense.

Acknowledgments

We thank Drs. Ashish Jain (National Institute of Allergy and Infectious Diseases (NIAID), Bethesda, MD), Warren Strober (NIAID, Bethesda, MD), and Barbara Mittleman (National Institute of Arthritis and Musculoskeletal and Skin Diseases (NIAMS), Bethesda, MD) for providing the HED-ID patients samples; Dr. Jack Yanovsky (National Institute of Child Health and Human Development, Bethesda, MD) for the control samples; Dr. Martin Gellert (National Institute of Diabetes and Digestive and Kidney Diseases, Bethesda, MD) for helpful discussions while preparing the manuscript; and Colleen Satorius (NIAMS, Bethesda, MD) and Randy Fisher (NIAMS, Bethesda, MD) for technical assistance.

Disclosures

The authors have no financial conflict of interest.

References

1. Kouskoff, V., and D. Nemazee. 2001. Role of receptor editing and revision in shaping the B and T lymphocyte repertoire. *Life Sci.* 69: 1105–1113.
2. Sen, R. 2006. Control of B lymphocyte apoptosis by the transcription factor NF-κB. *Immunity* 25: 871–883.
3. Thomas, M. D., B. Srivastava, and D. Allman. 2006. Regulation of peripheral B cell maturation. *Cell. Immunol.* 239: 92–102.
4. Gellert, M. 2002. V(D)J recombination: RAG proteins, repair factors, and regulation. *Annu. Rev. Biochem.* 71: 101–132.
5. Nemazee, D. 2000. Receptor selection in B and T lymphocytes. *Annu. Rev. Immunol.* 18: 19–51.
6. Caamano, J. H., C. A. Rizzo, S. K. Durham, D. S. Barton, C. Raventos-Suarez, C. M. Snapper, and R. Bravo. 1998. Nuclear factor (NF)-κ B2 (p100/p52) is required for normal splenic microarchitecture and B cell-mediated immune responses. *J. Exp. Med.* 187: 185–196.
7. Doi, T. S., T. Takahashi, O. Taguchi, T. Azuma, and Y. Obata. 1997. NF-κB RelA-deficient lymphocytes: normal development of T cells and B cells, impaired production of IgA and IgG1 and reduced proliferative responses. *J. Exp. Med.* 185: 953–961.
8. Enzler, T., G. Bonizzi, G. J. Silverman, D. C. Otero, G. F. Widhopf, A. Anzelon-Mills, R. C. Rickert, and M. Karin. 2006. Alternative and classical NF-κB signaling retain autoreactive B cells in the splenic marginal zone and result in lupus-like disease. *Immunity* 25: 403–415.
9. Gerondakis, S., R. Grumont, I. Rourke, and M. Grossmann. 1998. The regulation and roles of Rel/NF-κB transcription factors during lymphocyte activation. *Curr. Opin. Immunol.* 10: 353–359.
10. Grumont, R. J., I. J. Rourke, L. A. O'Reilly, A. Strasser, K. Miyake, W. Sha, and S. Gerondakis. 1998. B lymphocytes differentially use the Rel and nuclear factor κB1 (NF-κB1) transcription factors to regulate cell cycle progression and apoptosis in quiescent and mitogen-activated cells. *J. Exp. Med.* 187: 663–674.
11. Snapper, C. M., P. Zelazowski, F. R. Rosas, M. R. Kehry, M. Tian, D. Baltimore, and W. C. Sha. 1996. B cells from p50/NF-κB knockout mice have selective defects in proliferation, differentiation, germ-line CH transcription, and Ig class switching. *J. Immunol.* 156: 183–191.
12. Wu, M., H. Lee, R. E. Bellas, S. L. Schauer, M. Arsura, D. Katz, M. J. FitzGerald, T. L. Rothstein, D. H. Sherr, and G. E. Sonenshein. 1996. Inhibition of NF-κB/Rel induces apoptosis of murine B cells. *EMBO J.* 15: 4682–4690.
13. Bendall, H. H., M. L. Sikes, D. W. Ballard, and E. M. Oltz. 1999. An intact NF-κB signaling pathway is required for maintenance of mature B cell subsets. *Mol. Immunol.* 36: 187–195.
14. Verkoczy, L., D. Ait-Azzouzene, P. Skog, A. Martensson, J. Lang, B. Duong, and D. Nemazee. 2005. A role for nuclear factor κB/*rel* transcription factors in the regulation of the recombinase activator genes. *Immunity* 22: 519–531.
15. Combriato, G., and H. G. Klobeck. 2002. Regulation of human Ig lambda light chain gene expression by NF-κB. *J. Immunol.* 168: 1259–1266.
16. Demengeot, J., E. M. Oltz, and F. W. Alt. 1995. Promotion of V(D)J recombinational accessibility by the intronic E κ element: role of the κ B motif. *Int. Immunol.* 7: 1995–2003.
17. Hagman, J., C. M. Rudin, D. Haasch, D. Chaplin, and U. Storb. 1990. A novel enhancer in the immunoglobulin lambda locus is duplicated and functionally independent of NF κB. *Genes Dev.* 4: 978–992.

18. Heckman, C. A., T. Cao, L. Somsouk, H. Duan, J. W. Mehew, C. Y. Zhang, and L. M. Boxer. 2003. Critical elements of the immunoglobulin heavy chain gene enhancers for deregulated expression of bcl-2. *Cancer Res.* 63: 6666–6673.
19. Kanda, K., H. M. Hu, L. Zhang, J. Grandchamps, and L. M. Boxer. 2000. NF-κB activity is required for the deregulation of c-*myc* expression by the immunoglobulin heavy chain enhancer. *J. Biol. Chem.* 275: 32338–32346.
20. Wang, J., and L. M. Boxer. 2005. Regulatory elements in the immunoglobulin heavy chain gene 3′-enhancers induce c-*myc* deregulation and lymphomagenesis in murine B cells. *J. Biol. Chem.* 280: 12766–12773.
21. Bendall, H. H., M. L. Sikes, and E. M. Oltz. 2001. Transcription factor NF-κB regulates Ig lambda light chain gene rearrangement. *J. Immunol.* 167: 264–269.
22. Scherer, D. C., J. A. Brockman, H. H. Bendall, G. M. Zhang, D. W. Ballard, and E. M. Oltz. 1996. Corepression of RelA and c-*rel* inhibits immunoglobulin kappa gene transcription and rearrangement in precursor B lymphocytes. *Immunity* 5: 563–574.
23. Zelazowski, P., D. Carrasco, F. R. Rosas, M. A. Moorman, R. Bravo, and C. M. Snapper. 1997. B cells genetically deficient in the c-*Rel* transactivation domain have selective defects in germline CH transcription and Ig class switching. *J. Immunol.* 159: 3133–3139.
24. Tsai, C. L., A. H. Drejer, and D. G. Schatz. 2002. Evidence of a critical architectural function for the RAG proteins in end processing, protection, and joining in V(D)J recombination. *Genes Dev.* 16: 1934–1949.
25. Besmer, E., J. Mansilla-Soto, S. Cassard, D. J. Sawchuk, G. Brown, M. Sadofsky, S. M. Lewis, M. C. Nussenzweig, and P. Cortes. 1998. Hairpin coding end opening is mediated by RAG1 and RAG2 proteins. *Mol. Cell* 2: 817–828.
26. Ramsden, D. A., and M. Gellert. 1995. Formation and resolution of double-strand break intermediates in V(D)J rearrangement. *Genes Dev.* 9: 2409–2420.
27. Kenter, A. L., and J. Tredup. 1991. High expression of a 3′–5′ exonuclease activity is specific to B lymphocytes. *Mol. Cell. Biol.* 11: 4398–4404.
28. Lewis, S., A. Gifford, and D. Baltimore. 1985. DNA elements are asymmetrically joined during the site-specific recombination of κ immunoglobulin genes. *Science* 228: 677–685.
29. Schlissel, M. S. 1998. Structure of nonhairpin coding-end DNA breaks in cells undergoing V(D)J recombination. *Mol. Cell. Biol.* 18: 2029–2037.
30. Zhu, L., and B. D. Halligan. 1999. Characterization of a 3′–5′ exonuclease associated with VDJP. *Biochem. Biophys. Res. Commun.* 259: 262–270.
31. Courtois, G., and T. D. Gilmore. 2006. Mutations in the NF-κB signaling pathway: implications for human disease. *Oncogene* 25: 6831–6843.
32. Doffinger, R., A. Smahi, C. Bessia, F. Geissmann, J. Feinberg, A. Durandy, C. Bodemer, S. Kenwrick, S. Dupuis-Girod, S. Blanche, et al. 2001. X-linked anhidrotic ectodermal dysplasia with immunodeficiency is caused by impaired NF-κB signaling. *Nat. Genet.* 27: 277–285.
33. Filipe-Santos, O., J. Bustamante, M. H. Haverkamp, E. Vinolo, C. L. Ku, A. Puel, D. M. Frucht, K. Christel, H. von Bernuth, E. Jouanguy, et al. 2006. X-linked susceptibility to mycobacteria is caused by mutations in NEMO impairing CD40-dependent IL-12 production. *J. Exp. Med.* 203: 1745–1759.
34. Fusco, F., T. Bardaro, G. Fimiani, V. Mercadante, M. G. Miano, G. Falco, A. Israel, G. Courtois, M. D'Urso, and M. V. Ursini. 2004. Molecular analysis of the genetic defect in a large cohort of IP patients and identification of novel NEMO mutations interfering with NF-κB activation. *Hum. Mol. Genet.* 13: 1763–1773.
35. Jain, A., C. A. Ma, S. Liu, M. Brown, J. Cohen, and W. Strober. 2001. Specific missense mutations in NEMO result in hyper-IgM syndrome with hypohydrotic ectodermal dysplasia. *Nat. Immunol.* 2: 223–228.
36. Orange, J. S., A. Jain, Z. K. Ballas, L. C. Schneider, R. S. Geha, and F. A. Bonilla. 2004. The presentation and natural history of immunodeficiency caused by nuclear factor κB essential modulator mutation. *J. Allergy Clin. Immunol.* 113: 725–733.
37. Orange, J. S., O. Levy, and R. S. Geha. 2005. Human disease resulting from gene mutations that interfere with appropriate nuclear factor-κB activation. *Immunol. Rev.* 203: 21–37.
38. Hacker, H., and M. Karin. 2006. Regulation and function of IKK and IKK-related kinases. *Sci. STKE* 2006: re13.
39. Perkins, N. D. 2007. Integrating cell-signalling pathways with NF-κB and IKK function. *Nat. Rev. Mol. Cell. Biol.* 8: 49–62.
40. Solt, L. A., L. A. Madge, J. S. Orange, and M. J. May. 2007. Interleukin-1-induced NF-κB activation is NEMO-dependent but does not require IKKβ. *J. Biol. Chem.* 282: 8724–8733.
41. Zhao, T., L. Yang, Q. Sun, M. Arguello, D. W. Ballard, J. Hiscott, and R. Lin. 2007. The NEMO adaptor bridges the nuclear factor-κB and interferon regulatory factor signaling pathways. *Nat. Immunol.* 8: 592–600.
42. Agou, F., F. Traincard, E. Vinolo, G. Courtois, S. Yamaoka, A. Israel, and M. Veron. 2004. The trimerization domain of NEMO is composed of the interacting C-terminal CC2 and LZ coiled-coil subdomains. *J. Biol. Chem.* 279: 27861–27869.
43. Makris, C., J. L. Roberts, and M. Karin. 2002. The carboxyl-terminal region of IκB kinase γ (IKKγ) is required for full IKK activation. *Mol. Cell. Biol.* 22: 6573–6581.
44. Yang, F., J. Yamashita, E. Tang, H. L. Wang, K. Guan, and C. Y. Wang. 2004. The zinc finger mutation C417R of I-κB kinase γ impairs lipopolysaccharide- and TNF-mediated NF-κB activation through inhibiting phosphorylation of the I-κB kinase β activation loop. *J. Immunol.* 172: 2446–2452.
45. Vinolo, E., H. Sebban, A. Chaffotte, A. Israel, G. Courtois, M. Veron, and F. Agou. 2006. A point mutation in NEMO associated with anhidrotic ectodermal dysplasia with immunodeficiency pathology results in destabilization of the oligomer and reduces lipopolysaccharide- and tumor necrosis factor-mediated NF-κB activation. *J. Biol. Chem.* 281: 6334–6348.
46. Souto-Carneiro, M. M., N. S. Longo, D. E. Russ, H. W. Sun, and P. E. Lipsky. 2004. Characterization of the human Ig heavy chain antigen binding complementarity determining region 3 using a newly developed software algorithm, JOINSOLVER. *J. Immunol.* 172: 6790–6802.
47. Souto-Carneiro, M. M., G. P. Sims, H. Girschik, J. Lee, and P. E. Lipsky. 2005. Developmental changes in the human heavy chain CDR3. *J. Immunol.* 175: 7425–7436.
48. Sasaki, Y., E. Derudder, E. Hobeika, R. Pelanda, M. Reth, K. Rajewsky, and M. Schmidt-Supprian. 2006. Canonical NF-κB activity, dispensable for B cell development, replaces BAFF-receptor signals and promotes B cell proliferation upon activation. *Immunity* 24: 729–739.
49. Pasparakis, M., M. Schmidt-Supprian, and K. Rajewsky. 2002. IκB kinase signaling is essential for maintenance of mature B cells. *J. Exp. Med.* 196: 743–752.
50. Jain, A., C. A. Ma, E. Lopez-Granados, G. Means, W. Brady, J. S. Orange, S. Liu, S. Holland, and J. M. Derry. 2004. Specific NEMO mutations impair CD40-mediated c-Rel activation and B cell terminal differentiation. *J. Clin. Invest.* 114: 1593–1602.
51. Liou, H. C., W. C. Sha, M. L. Scott, and D. Baltimore. 1994. Sequential induction of NF-κB/Rel family proteins during B-cell terminal differentiation. *Mol. Cell. Biol.* 14: 5349–5359.
52. Kim, S., R. N. La Motte-Mohs, D. Rudolph, J. C. Zuniga-Pflucker, and T. W. Mak. 2003. The role of nuclear factor-κB essential modulator (NEMO) in B cell development and survival. *Proc. Natl. Acad. Sci. USA* 100: 1203–1208.
53. Patterson, H. C., M. Kraus, Y. M. Kim, H. Ploegh, and K. Rajewsky. 2006. The B cell receptor promotes B cell activation and proliferation through a non-ITAM tyrosine in the Igα cytoplasmic domain. *Immunity* 25: 55–65.
54. Wang, L., R. Wuerffel, and A. L. Kenter. 2006. NF-κB binds to the immunoglobulin Sγ3 region in vivo during class switch recombination. *Eur. J. Immunol.* 36: 3315–3323.
55. Horwitz, B. H., P. Zelazowski, Y. Shen, K. M. Wolcott, M. L. Scott, D. Baltimore, and C. M. Snapper. 1999. The p65 subunit of NF-κB is redundant with p50 during B cell proliferative responses, and is required for germline C_H transcription and class switching to IgG3. *J. Immunol.* 162: 1941–1946.
56. Sepulveda, M. A., A. V. Emelyanov, and B. K. Birshtein. 2004. NF-κB and Oct-2 synergize to activate the human 3′ Igh hs4 enhancer in B cells. *J. Immunol.* 172: 1054–1064.
57. Sha, W. C., H. C. Liou, E. I. Tuomanen, and D. Baltimore. 1995. Targeted disruption of the p50 subunit of NF-κB leads to multifocal defects in immune responses. *Cell* 80: 321–330.
58. O'Brien, D. P., E. M. Oltz, and B. G. Van Ness. 1997. Coordinate transcription and V(D)J recombination of the κ immunoglobulin light-chain locus: NF-κB-dependent and -independent pathways of activation. *Mol. Cell. Biol.* 17: 3477–3487.
59. Busslinger, M. 2004. Transcriptional control of early B cell development. *Annu. Rev. Immunol.* 22: 55–79.
60. Collins, A. M., M. Ikutani, D. Puiu, G. A. Buck, A. Nadkarni, and B. Gaeta. 2004. Partitioning of rearranged Ig genes by mutation analysis demonstrates D-D fusion and V gene replacement in the expressed human repertoire. *J. Immunol.* 172: 340–348.
61. Sanz, I. 1991. Multiple mechanisms participate in the generation of diversity of human H chain CDR3 regions. *J. Immunol.* 147: 1720–1729.
62. Klein, U., K. Rajewsky, and R. Kuppers. 1999. Phenotypic and molecular characterization of human peripheral blood B-cell subsets with special reference to N-region addition and Jκ-usage in Vκ Jκ-joints and κ/λ-ratios in naive versus memory B-cell subsets to identify traces of receptor editing processes. *Curr. Top. Microbiol. Immunol.* 246: 141–146, discussion 147.
63. Tian, C., G. K. Luskin, K. M. Dischert, J. N. Higginbotham, B. E. Shepherd, and J. E. Crowe, Jr. 2007. Evidence for preferential Ig gene usage and differential TdT and exonuclease activities in human naive and memory B cells. *Mol. Immunol.* 44: 2173–2183.
64. Mansilla-Soto, J., and P. Cortes. 2003. VDJ recombination: Artemis and its in vivo role in hairpin opening. *J. Exp. Med.* 197: 543–547.
65. Niewolik, D., U. Pannicke, H. Lu, Y. Ma, L. C. Wang, P. Kulesza, E. Zandi, M. R. Lieber, and K. Schwarz. 2006. DNA-PKcs dependence of Artemis endonucleolytic activity, differences between hairpins and 5′ or 3′ overhangs. *J. Biol. Chem.* 281: 33900–33909.
66. Cobaleda, C., A. Schebesta, A. Delogu, and M. Busslinger. 2007. Pax5: the guardian of B cell identity and function. *Nat. Immunol.* 8: 463–470.
67. Ivanov, II, R. L. Schelonka, Y. Zhuang, G. L. Gartland, M. Zemlin, and H. W. Schroeder, Jr. 2005. Development of the expressed Ig CDR-H3 repertoire is marked by focusing of constraints in length, amino acid use, and charge that are first established in early B cell progenitors. *J. Immunol.* 174: 7773–7780.
68. Klein, U., K. Rajewsky, and R. Kuppers. 1998. Human immunoglobulin (Ig)M^+IgD^+ peripheral blood B cells expressing the CD27 cell surface antigen carry somatically mutated variable region genes: CD27 as a general marker for somatically mutated (memory) B cells. *J. Exp. Med.* 188: 1679–1689.